THE JOURNAL OF PHYSICAL CHEMISTRY C

Article

pubs.acs.org/JPCC

Blocking Hot Electron Emission by SiO_2 Coating Plasmonic Nanostructures

Nobuyuki Takeyasu,[*,†,§] Kenzo Yamaguchi,[*,‡,∥,§] Ryusuke Kagawa,[†] Takashi Kaneta,[†] Felix Benz,[∥] Masamitsu Fujii,[⊥] and Jeremy J. Baumberg[∥]

[†]Graduate School of Natural Science and Technology, Okayama University, 3-1-1 Tsushima-naka, Kita-ku, Okayama 700-8530, Japan

[‡]Department of Advanced Materials Science, Faculty of Engineering, Kagawa University, 2217-20 Hayashi-cho, Takamatsu, Kagawa 761-0396, Japan

[∥]NanoPhotonics Centre, Cavendish Laboratory, Department of Physics, University of Cambridge, J.J. Thomson Avenue, Cambridge CB3 0HE, United Kingdom

[⊥]Department of Electronics and Mechanics, Toba National College of Maritime Technology, 1-1 Ikegami-cho, Toba, Mie 517-8501, Japan

ABSTRACT: Noble metallic nanostructures provide a platform for high-sensitivity spectroscopic sensing with significantly enhanced electromagnetic fields due to surface plasmon polaritons. However, target molecules can be transformed into other molecules under irradiation with an excitation laser during the surface-enhanced measurement, which thus disturbs detection of unknown samples. In this paper, we perform Raman measurements of *p*-aminothiophenol on gold nanosurfaces with and without deposition of SiO_2 thin films at the surface. The Raman signals are enhanced on both substrates, but the deposition of the glass thin film clearly prevents the chemical transformation. This indicates that hot electrons are effective for chemical transformation and that thin glass films are sufficient to prevent this while still benefiting from surface plasmons.

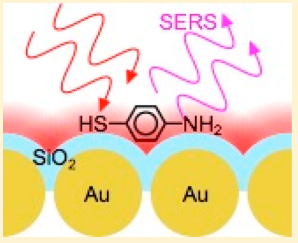

1. INTRODUCTION

Noble metallic nanostructures, typically made of gold or silver, can support localized surface plasmon polaritons which can confine light to the structure surface and thereby locally boost the electric field intensity. This local enhancement makes such structures ideal platforms for high-sensitivity spectroscopic sensing methods, such as surface-enhanced Raman spectroscopy (SERS), tip-enhanced Raman spectroscopy (TERS), and enhanced fluorescence techniques.[1−3] SERS is based on the enhancement of field E for the Raman process ($\propto |E|^4$): already a modest field enhancement of just 10 therefore leads to a 10 000-fold enhancement of the Raman signal. Surface-enhanced Raman signals were first observed for molecules bound to rough silver electrodes[4−6] but has rapidly evolved to inspire novel platforms that push detection limits and fundamental investigations.[7−13]

One of the main benefits of SERS is the ability to directly study chemical reactions on the few molecule scale. A favored molecule in this context *p*-aminothiophenol (*p*-ATP) adsorbs at the metallic surface through formation of metal−thiol bonds and can therefore be easily assembled in the desired geometry.[14−18] In the presence of gold and silver nanostructures it undergoes a chemical reaction forming dimercaptoazobenzene (DMAB), which is characterized by the appearance of three new SERS peaks at 1140, 1389, and 1433 cm^{-1}, which correspond to the A_{1g} modes of DMAB.[19−22] The transformation of *p*-ATP to DMAB is widely believed to be due to the emission of hot electrons from the plasmonic nanostructures,[23−28] which are generated during the decay of the surface plasmons (LSPPs).

We studied the chemical transformation of *p*-ATP on a highly uniform silver nanoparticle array using a 532 nm laser. The chemical transformation from *p*-ATP to DMAB was observed for laser intensities greater than ∼19 W/mm^2 (enhancement factor > 10^4).[22] In contrast, no Raman signal of DMAB could be observed without the silver nanosurface even for laser intensities as high as 467 W/mm^2, since no chemical transformation occurred. Alternative reaction mechanisms might involve heating caused by plasmon absorption, since the speed of chemical reactions increases exponentially with temperature. It is also known that noble metals work as catalytic materials, reducing the activation energy.[29−31] Noble metal nanosurfaces thus exhibit a dual functionality, which is both plasmonic and catalytic, and can be initiated during SERS measurement.

Our aim here is to separate the catalytic activity of plasmonic nanostructures from their SERS activity by using a 5 nm thick silicon dioxide (SiO_2) layer. Similarly, thin SiO_2 was coated on AuNPs for SHINERS, where the SiO_2 coating enabled AuNPs to spread over the probed surface.[32] This layer blocks hot electrons from reaching the *p*-ATP molecules but lets the electromagnetic field penetrate, allowing us to measure the

Received: March 12, 2017
Revised: July 9, 2017
Published: August 2, 2017

DOI: 10.1021/acs.jpcc.7b02345
J. Phys. Chem. C 2017, 121, 18795−18799

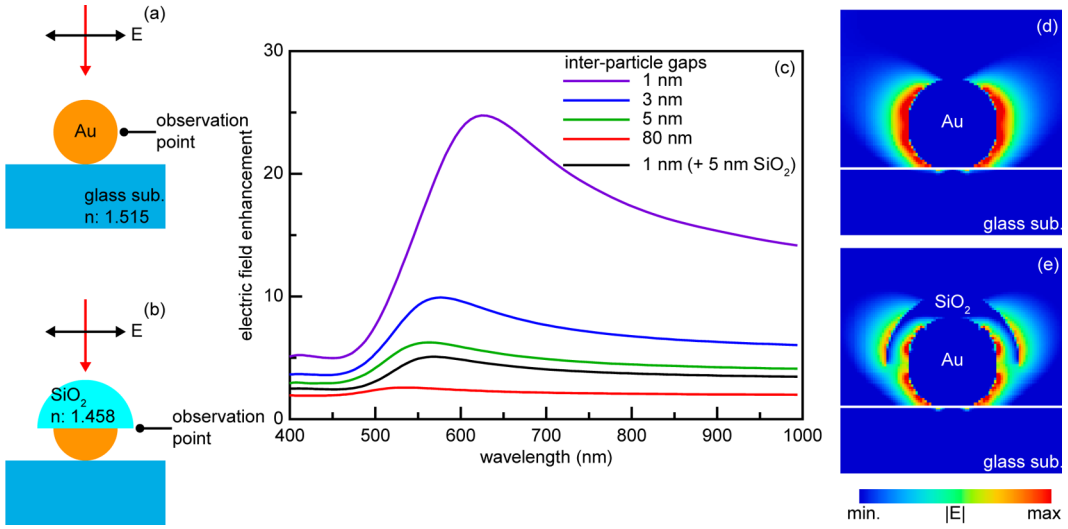

Figure 1. Unit structures for FDTD simulations: 20 nm AuNP (a) without and (b) with 5 nm thick SiO_2. (c) Electric field enhancement ($|E|/|E_{inc}|$) at interparticle gaps of 1, 3, 5, and 80 nm for bare AuNP and 1 nm for AuNP capped with 5 nm SiO_2. Electric field distributions of (d) AuNP (5 nm gap) and (e) AuNP capped with 5 nm SiO_2 (1 nm gap).

SERS of the monomer without triggering a chemical reaction. The SERS measurement was performed at 633 nm on two-dimensional gold nanoparticle (2D AuNP) arrays covered with/without thin SiO_2. Gold is used because of its chemical stability, although higher enhancement is expected with silver.

2. EXPERIMENTAL SECTION

2.1. Materials. *n*-Octylamine (C8: $C_8H_{17}NH_2$) was purchased from Tokyo Chemical Industry. *n*-Hexane was purchased from Kanto Chemical. Sodium tetrachloroaurate(III) dihydrate ($HAuCl_4{\cdot}2H_2O$), trisodium citrate dihydrate ($C_6H_5Na_3O_7{\cdot}2H_2O$), and *p*-aminothiophenol ($H_2NC_6H_4SH$) were purchased from Wako Pure Chemical Industries. Deionized water was used in all experiments. All glass slides were cleaned several times by ultrasonication of ethanol, water, and acetone.

2.2. Synthesis of Citrate-Capped AuNPs. AuNPs were synthesized as reported in ref 33. A 100 mL amount of deionized water, 500 μL of a 50 mM $NaAuCl_4$ solution, and 3.5 mL of 3% (w/v) citrate solution were mixed in a sample bottle, and the mixture was heated to 80 °C for 3 h. The initially yellow solution changed its color first to dark-blue and subsequently to red. The AuNPs solution was cooled to room temperature.

2.3. Fabrication of SERS Substrate. The details about the fabrication method of SERS substrate have been reported in ref 34. In brief, a 300 μL amount of 20 mM *n*-octylamine (C8) in *n*-hexane solution and 18 mL of water were mixed in a beaker. A 6 mL amount of the prepared AuNPs solution was added to the resulting emulsion. Subsequently, a glass slide was immersed in the solution, and an appropriate amount of *n*-hexane to cover the whole surface was added. The color of the aqueous phase disappeared, indicating that a 2D AuNP array was formed at the oil/water interface. The glass slide was pulled up from the solution using a dip coater (SDI, ND-0407-S3: Kagawa University, 20 μm/s), and thereby the AuNP array was transferred to the glass surface.

2.4. Coating SERS Substrate with SiO_2. The SERS substrate (AuNP/glass) was coated with SiO_2 of 5 nm thickness (SiO_2/AuNP/glass) by using a dual-ion beam sputtering system (Hashinotech, 10W-IBS: Kagawa University) under a pressure of 6.0×10^{-4} Pa.

2.5. Measurement of Extinction Spectrum and SERS. Extinction spectra of AuNP solutions and the SERS substrates were measured by an absorption photometer (Shimadzu, UV-2400PC and SolidSpec-3700: Kagawa University).

The SERS substrate was washed with deionized water and ethanol alternately and dried before SERS measurement. A 10 μL amount of 1 mM *p*-aminothiophenol (*p*-ATP) in ethanol solution was cast and dried on the SERS substrate and covered with SiO_2. We performed the SERS measurement of *p*-ATP on each SERS substrate using a micro-Raman spectrometer (Renishaw inVia Raman Microscope: University of Cambridge). The wavelength of the excitation laser was 632.8 nm (He−Ne laser), and the output power was 2.31 mW. The objective lens with a numerical aperture (NA) of 0.40 and magnification of ×20 focused the excitation laser (spot diameter 1.93 μm) and collected Raman scattering from the sample. The exposure time was 1 s. All SERS spectra were normalized by the substrate spectrum using

$$\text{Raman spectrum} = \text{original spectrum(OS)} - \frac{\text{substrate spectrum} \times \text{max value(OS)}}{\text{max}} \quad (1)$$

3. RESULTS AND DISCUSSION

3.1. Calculation of Electric Field on AuNPs Capped with 5 nm Thick SiO_2 Layer. The attenuation of the electric field due to the 5 nm thick SiO_2 layer was evaluated with finite-difference time domain (FDTD) methods. Figure 1a and 1b shows the two unit structures, 20 nm AuNP without and with 5 nm SiO_2, respectively, and each structure was tessellated periodically in a square pattern using different interparticle gaps. We used a capped structure for AuNP with SiO_2 since it was reported that the cap structures were fabricated with vacuum evaporation.[35,36] Plane waves were illuminated from the top, with polarization parallel to the substrate. Figure 1c shows the relationship between the electric field enhancement ($|E|/|E_{inc}|$) and the excitation wavelength with different

DOI: 10.1021/acs.jpcc.7b02345
J. Phys. Chem. C 2017, 121, 18795−18799

interparticle gaps of 1, 3, 5, and 80 nm for a 20 nm AuNP square array. The peak intensity increases, and its spectral position red shifts as the interparticle gap decreases. The electric fields on AuNPs capped with 5 nm SiO_2 (for interparticle gap of 1 nm) were calculated, also shown in Figure 1c. The field enhancements on these structures are similar, which means that attenuation of the electric field was small due to the extra 5 nm thick SiO_2. Enhancements of the electric field are almost comparable in these cases.

Figure 1d and 1e shows the electric field distributions of the two unit structures at 532 nm showing their similarity. These simulations thus suggest that 5 nm thick SiO_2 will still allow steady-state SERS measurements.

3.2. Evaluation of SERS Substrates. Figure 2a shows schematics of the prepared samples, which are AuNP array

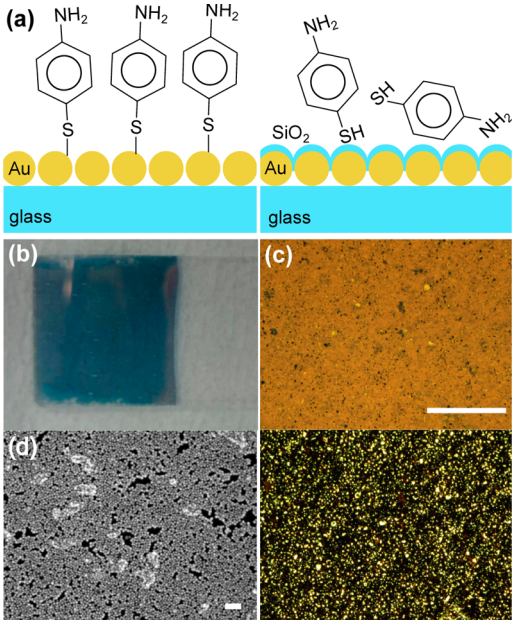

Figure 2. (a) Schematics of cross-section of samples: *p*-ATP on AuNP array without (left) and with (right) SiO_2 layer. (b) Photograph, (c) bright-field (top) and dark-field (bottom) optical microscopic images, and (d) SEM image of 2D AuNP array. Scale bars in c and d indicate 0.5 mm and 100 nm, respectively.

substrates with and without SiO_2 coating. The *p*-ATPs are randomly oriented on the SiO_2 layer but bound to the Au particles by the thiol group. The SiO_2 layer blocks the emission of hot electrons during the laser illumination. Figure 2b shows a photograph of the sample. The size of the 2D AuNP array is 26 × 26 mm, and the color is uniformly blue over the whole array structure. We characterize the 2D AuNP array with an optical microscope (20× , NA = 0.40). Figure 2c shows optical microscopic reflection images of the 2D AuNP array in bright and dark field. An orange color (complementary to blue of Figure 2b) is observed over the whole array in bright field, and the image was found to be relatively uniform over the whole structure, although some local points show defects. The dark-field image shows yellow scattered light from these defects on the surface of the assembled nanoparticle array. Figure 2d shows a SEM image of the 2D AuNP array, which is a monolayer composed of 20 nm AuNPs, which are sufficiently close to each other to exhibit a hybrid plasmon resonance,[37] although some defects of around 100 nm size are found.

Figure 3 shows extinction spectra of AuNP arrays. The extinction spectra of the 2D AuNP arrays are red shifted (650

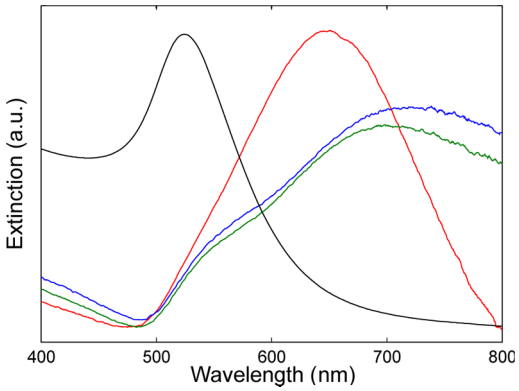

Figure 3. Extinction spectra of AuNP array (red), SiO_2-coated AuNP array (green), *p*-ATP on SiO_2-coated AuNP array (blue), and AuNP solution of monomers (black). Thickness of SiO_2 layer is 5 nm.

nm) with respect to the single-particle spectra (522 nm), indicating that the individual nanoparticles are sufficiently close to allow coupling of the LSPPs (alkane length is <2.2 nm).[34,38,39] Depositing the 5 nm thick layer of SiO_2 on top leads to a further red shift of approximately 90 nm (to 740 nm) due to the increased refractive index. Additional coating of the structure with the target molecule *p*-ATP (which binds now by physical adsorption), causes a further small red shift of the extinction peak and peak broadening due to the difference of the refractive index between air and *p*-ATP.

3.3. Effect of SiO_2 Layer on SERS Measurement. The SERS spectrum of *p*-ATP on the bare 2D AuNP array (*p*ATP/AuNPs/glass) is shown in Figure 4 (800 W/mm^2, 633 nm laser). Strong Raman peaks are observed at 1074, 1138, 1389,

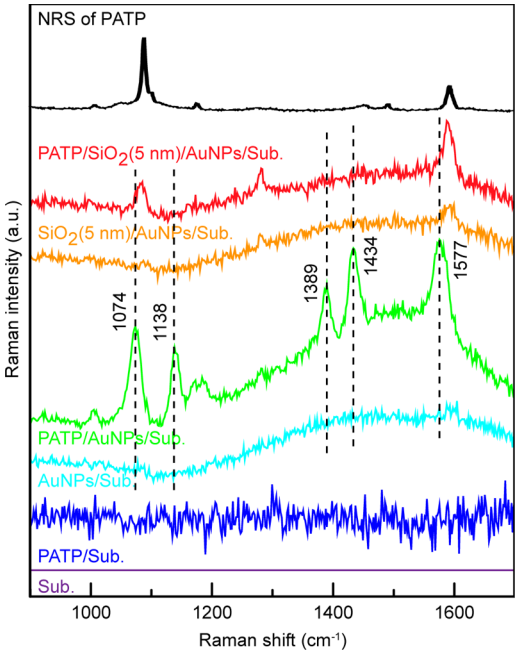

Figure 4. Raman spectra of glass Substrate (Sub., purple), PATP/Sub. (blue), AuNP/Sub. (cyan), PATP/AuNP/Sub. (green), SiO_2/AuNP/Sub. (orange), PATP/SiO_2/AuNP/Sub. (red), and normal Raman spectrum of PATP (black).

DOI: 10.1021/acs.jpcc.7b02345
J. Phys. Chem. C 2017, 121, 18795−18799

1434, and 1577 cm^{-1} with a broad background ranging from 1200 to 1700 cm^{-1}. These lines indicate that *p*-ATP has reacted to give DMAB. The broad background originates from the scattering of the 2D AuNP array and is also observed in the spectrum of AuNPs/Sub, although not from the bare glass substrate (Sub.) whether *p*-ATP coated or not. These control experiments show no Raman peaks, indicating that the AuNP monolayer substrate is necessary to observe the SERS spectra. In addition to the three Raman peaks which are characteristic for DMBA (1138, 1389, and 1434 cm^{-1}) some weak SERS peaks are observed which are also present for the bare 2D AuNP array, indicating that these peaks are due to remaining reactants in the nanoparticle solution. We note that the laser intensity used (~800 W/mm^2) is much larger than reported to be required to trigger the chemical reaction of *p*-ATP to DMAB (~20 W/mm^2) in order to make sure that the reaction occurs.[18,22]

In order to stop the chemical reaction from occurring we deposit a 5 nm thick SiO_2 layer between the 2D AuNP array and the analyte layer (PATP/SiO_2/AuNP/Sub.). This layer blocks the hot electrons from reaching the *p*-ATP layer. We observe that the three peaks of DMAB disappear, and the only Raman peaks are found at 1078, 1280, and 1582 cm^{-1}, although the laser power is larger than the threshold for the chemical transformation by more than 50 times. The bare SiO_2-coated AuNP array (SiO_2/AuNP/Sub.) shows the same two small peaks as the AuNP/Sub. structure (1280 and 1582 cm^{-1}), which originate from *n*-octylamine adsorbed onto the surface of the AuNPs during fabrication of the 2D AuNP array. Our results clearly show Raman peaks from *p*-ATP even when using the SiO_2 spacer between the 2D AuNP array and the *p*-ATP layer—the electromagnetic fields can penetrate the spacer layer and still lead to sizable SERS enhancements. This result highlights that the enhanced electromagnetic fields alone are not sufficient to trigger the *p*-ATP to DMAB reaction but that rather a direct contact with the noble metal structure is required. Catalysis due to plasmonic heating is not dominating here, as heat can still be easily transported across the thin spacer layer.

4. CONCLUSION

In conclusion, we have shown SERS measurements of *p*-ATP on a 2D AuNP array with and without deposition of a thin SiO_2 layer. This layer acts as a filter allowing electromagnetic fields to penetrate but blocking hot electrons from reaching the molecules. As a result, Raman peaks of DMAB are observed without the SiO_2 layer but are completely absent when the SiO_2 layer is added. These results indicate that deposition of SiO_2 on Au nanosurfaces allows SERS measurements of target molecules without chemical transformation. Our results also indicate that the *p*-ATP to DMAB reaction is indeed driven by hot electrons (which are blocked by the glass layer) and not by heat or the enhanced electromagnetic fields (which penetrate the glass layer).

AUTHOR INFORMATION

Corresponding Authors

*E-mail: takeyasu@okayama-u.ac.jp.

*E-mail: kenzo@eng.kagawa-u.ac.jp.

ORCID

Nobuyuki Takeyasu: 0000-0001-7221-1606

Takashi Kaneta: 0000-0001-9076-3906

Jeremy J. Baumberg: 0000-0002-9606-9488

Author Contributions

§N.T. and K.Y. contributed equally to this work.

Notes

The authors declare no competing financial interest.

ACKNOWLEDGMENTS

This research was partly supported by The Yakumo Foundation for Environmental Science, JSPS KAKENHI under Grant No. 15H03546, and Nanotechnology Platform Program (Kagawa University) of the Ministry of Education, Culture, Sports, Science and Technology (MEXT), Japan, and the UK Engineering and Physical Sciences Research Council grants EP/G060649/1 and EP/L027151/1 and ERC grant LINASS 320503. F.B. acknowledges financial support from the Winton Programme for the Physics of Sustainability.

REFERENCES

(1) Kneipp, K.; Kneipp, H.; Itzkan, I.; Dasari, R. R.; Feld, M. S. Ultrasensitive chemical analysis by Raman spectroscopy. *Chem. Rev.* **1999**, *99*, 2957−2975.

(2) Stiles, P. L.; Dieringer, J. A.; Shah, N. C.; Van Duyne, R. P. Surface-enhanced Raman spectroscopy. *Annu. Rev. Anal. Chem.* **2008**, *1*, 601−626.

(3) Fort, E.; Gresillon, S. Surface Enhanced Fluorescence. *J. Phys. D: Appl. Phys.* **2008**, *41*, 013001.

(4) Fleischmann, M.; Hendra, P. J.; McQuillan, A. J. Raman spectra of pyridine adsorbed at a silver electrode. *Chem. Phys. Lett.* **1974**, *26*, 163−166.

(5) Albrecht, M. G.; Creighton, J. A. Anomalously intense Raman spectra of pyridine at a silver electrode. *J. Am. Chem. Soc.* **1977**, *99*, 5215−5217.

(6) Jeanmaire, D. L.; Van Duyne, R. P. Surface Raman spectroelectrochemistry part I. Heterocyclic, aromatic, and aliphatic amines adsorbed on the anodized silver electrode. *J. Electroanal. Chem. Interfacial Electrochem.* **1977**, *84*, 1−20.

(7) Nie, S. M.; Emory, S. R. Probing single molecules and single nanoparticles by surface-enhanced Raman scattering. *Science* **1997**, *275*, 1102−1106.

(8) Kneipp, K.; Wang, Y.; Kneipp, H.; Perelman, L. T.; Itzkan, I.; Dasari, R. R.; Feld, M. S. Single molecule detection using surface-enhanced Raman scattering (SERS). *Phys. Rev. Lett.* **1997**, *78*, 1667−1670.

(9) Emory, S. R.; Jensen, R. A.; Wenda, T.; Han, M.; Nie, S. Re-examining the origins of spectral blinking in single-molecule and single-nanoparticle SERS. *Faraday Discuss.* **2006**, *132*, 249−259.

(10) Manjavacas, A.; Abajo, F. J. G. d.; Nordlander, P. Quantum Plexcitonics: Strongly interacting plasmons and excitons. *Nano Lett.* **2011**, *11*, 2318−2323.

(11) Yamamoto, Y. S.; Ozaki, Y.; Itoh, T. Recent progress and frontiers in the electromagnetic mechanism of surface-enhanced Raman scattering. *J. Photochem. Photobiol., C* **2014**, *21*, 81−104.

(12) Itoh, T.; Yamamoto, Y. S.; Tamaru, H.; Biju, V.; Wakida, S.; Ozaki, Y. Single-molecular surface-enhanced resonance Raman scattering as a quantitative probe of local electromagnetic field: The case of strong coupling between plasmonic and excitonic resonance. *Phys. Rev. B: Condens. Matter Mater. Phys.* **2014**, *89*, 195436.

(13) Benz, F.; Tserkezis, C.; Herrmann, L. O.; de Nijs, B.; Sanders, A.; Sigle, D. O.; Pukenas, L.; Evans, S. D.; Aizpurua, J.; Baumberg, J. J. Nanooptics of molecular-shunted plasmonic nanojunctions. *Nano Lett.* **2015**, *15*, 669−674.

(14) Osawa, M.; Matsuda, N.; Yoshii, K.; Uchida, I. Charge transfer resonant Raman process in surface-enhanced Raman scattering from *p*-aminothiophenol adsorbed on silver: Herzberg-Teller contribution. *J. Phys. Chem.* **1994**, *98*, 12702−12707.

DOI: 10.1021/acs.jpcc.7b02345
J. Phys. Chem. C 2017, 121, 18795−18799

(15) Wang, Y.; Chen, H.; Dong, S.; Wang, E. Surface-enhanced Raman scattering of *p*-aminothiophenol self-assembled monolayers in sandwich structure fabricated on glass. *J. Chem. Phys.* **2006**, *124*, 074709.
(16) Wang, Y.; Zou, X.; Ren, W.; Wang, W.; Wang, E. Effect of silver nanoplates on Raman spectra of *p*-aminothiophenole assembled on smooth macroscopic gold and silver surface. *J. Phys. Chem. C* **2007**, *111*, 3259−3265.
(17) Baia, L.; Baia, M.; Popp, J.; Astilean, S. Gold films deposited over regular array of polystyrene nanospheres as highly effective SERS substrates from visible to NIR. *J. Phys. Chem. B* **2006**, *110*, 23982.
(18) Liu, G. K.; Hu, J.; Zheng, P. C.; Shen, G. L.; Jiang, J. H.; Yu, R. Q.; Cui, Y.; Ren, B. Laser-induced formation of metal-molecule-metal junctions between Au nanoparticles as probed by surface-enhanced Raman spectroscopy. *J. Phys. Chem. C* **2008**, *112*, 6499−6508.
(19) Huang, Y.-F.; Zhu, H.-P.; Liu, G. K.; Wu, D.-Y.; Ren, B.; Tian, Z.-Q. When the signal is not from the original molecule to be detected: Chemical transformation of *para*-aminothiophenol on Ag during the SERS. *J. Am. Chem. Soc.* **2010**, *132*, 9244−9246.
(20) Sun, M.; Huang, Y.; Xia, L.; Chen, X.; Xu, H. The pH-controlled plasmon-assisted surface photocatalysis reaction of 4-aminothiophenol to *p*,*p*′-dimercaptoazobenzene on Au, Ag, and Cu colloids. *J. Phys. Chem. C* **2011**, *115*, 9629−9636.
(21) Choi, H.-K.; Shon, H. K.; Yu, H.; Lee, T. G.; Kim, Z. H. b_2 peaks in SERS spectra of 4-aminobenzenthiol: A photochemical artifact or a real chemical enhancement? *J. Phys. Chem. Lett.* **2013**, *4*, 1079−1086.
(22) Takeyasu, N.; Kagawa, R.; Sakata, K.; Kaneta, T. Laser power threshold of chemical transformation on highly uniform plasmonic and catalytic nano-surface. *J. Phys. Chem. C* **2016**, *120*, 12163−12169.
(23) Liu, R.; He, Z.; Sun, J.; Liu, J.; Jiang, G. Tracking the fate of surface plasmon resonance-generated hot electrons by in situ SERS surveying of catalyzed reaction. *Small* **2016**, *12*, 6378−6387.
(24) Dong, B.; Fang, Y.; Chen, X.; Xu, H.; Sun, M. Substrate-, wavelength-, and time-dependent plasmon-assisted surface catalysis reaction of 4-nitrobenzenethiol dimerizing to *p*,*p*′-dimercaptoazobenzene on Au, Ag, and Cu films. *Langmuir* **2011**, *27*, 10677−10682.
(25) Tasi, T.-T.; Lin, T.-W.; Shao, L.-D.; Shen, H.-H. Reversible coupling of 4-nitroaniline molecules to 4-aminothiophenol functionalized on Ag nanoparticle/graphene oxide nanocomposites through the plasmon assisted chemical reaction. *RSC Adv.* **2016**, *6*, 29453−29459.
(26) Zhang, Z.; Deckert-Gaudig, T.; Singh, P.; Deckert, V. Single molecule level plasmonic catalysis - a dilution study of *p*-nitrothiophenol on gold dimers. *Chem. Commun.* **2015**, *51*, 3069−3072.
(27) Brandt, N. C.; Keller, E. L.; Frontiera, R. R. Ultrafast surface-enhanced Raman probing of the role of hot electrons in plasmon-driven chemistry. *J. Phys. Chem. Lett.* **2016**, *7*, 3179−3185.
(28) Park, J. Y.; Baker, L. R.; Somorjai, G. A. Role of hot electrons and metal-oxide interfaces in surface chemistry and catalytic reactions. *Chem. Rev.* **2015**, *115*, 2781−2817.
(29) Hashmi, A. S. K.; Hutchings, G. J. Gold Catalysis. *Angew. Chem., Int. Ed.* **2006**, *45*, 7896−7936.
(30) Lewis, L. N. Chemical Catalysis by Colloids and Clusters. *Chem. Rev.* **1993**, *93*, 2693−2730.
(31) Tsunoyama, H.; Sakurai, H.; Negishi, Y.; Tsukuda, T. Size-specific catalytic activity of polymer-stabilized gold nanoclusters for aerobic alcohol oxidation in water. *J. Am. Chem. Soc.* **2005**, *127*, 9374−9375.
(32) Li, J. F.; Huang, Y. F.; Ding, Y.; Yang, Z. L.; Li, S. B.; Zhou, X. S.; Fan, F. R.; Zhang, W.; Zhou, Z. Y.; Wu, D. Y.; et al. Shell-isolated nanoparticle-enhanced Raman spectroscopy. *Nature* **2010**, *464*, 392−395.
(33) Turkevich, J.; Stevenson, P. C.; Hillier, J. A study of the nucleation and growth processes in the synthesis of colloidal gold. *Discuss. Faraday Soc.* **1951**, *11*, 55−75.
(34) Kagawa, R.; Takeyasu, N.; Kaneta, T.; Takemoto, Y. Oil-in-water emulsion as fabrication platform for uniform plasmon-controlled two-dimensional metallic nanoparticle array. *Appl. Phys. Express* **2016**, *9*, 075003.
(35) Kim, H.; Takei, H.; Yasuda, K. Production of size-controlled nanoscopic cap-shaped metal shells. *Jpn. J. Appl. Phys.* **2010**, *49*, 048004.
(36) In *Progress in Nano-Electro-Optics III*; Ohtsu, M., Ed.; Springer: Verlag Berlin Heidelberg, Germany, 2005.
(37) Prodan, E.; Radloff, C.; Halas, N. J.; Nordlander, P. A hybridization model for the plasmon response of complex nanostructures. *Science* **2003**, *302*, 419−422.
(38) Chen, C.-F.; Tzeng, S.-D.; Chen, H.-Y.; Lin, K.-J.; Gwo, S. Tunable plasmonic response from alkanethiolate-stabilized gold nanoparticle superlattices: Evidence of near-field coupling. *J. Am. Chem. Soc.* **2008**, *130*, 824−826.
(39) Shin, Y.; Song, J.; Kim, D.; Kang, T. Facile preparation of ultrasmall void metallic nanogap from self-assembled gold−silica core−shell nanoparticles monolayer via kinetic control. *Adv. Mater.* **2015**, *27*, 4344−4350.

DOI: 10.1021/acs.jpcc.7b02345
J. Phys. Chem. C 2017, 121, 18795−18799